

Description of the larval instars of *Amidorus immaturus* (Mulsant, 1842) (Coleoptera: Scarabaeoidea: Aphodiidae)

Angela ROGGERO*, Claudia TOCCO, Claudia PALESTRINI

Department of Life Sciences and Systems Biology, University of Torino, I-10123 Torino, Italy

Received: 14.02.2012 • Accepted: 16.06.2012 • Published Online: 24.12.2012 • Printed: 21.01.2013

Abstract: The morphology of the 1st and 2nd larval instars of *A. immaturus* (Mulsant, 1842) is described and illustrated here for the first time, with an emphasis on the cephalic capsule, head appendages, legs, and last abdominal segments. The cephalic capsule size was employed to determine the larval instar, while the genital disc was employed to assess the sex of the larvae. The growth and sex ratio of *A. immaturus* were analyzed.

Key words: Dung beetles, Aphodiinae, *Amidorus immaturus*, larval instar, larval sex

1. Introduction

The widespread and heterogeneous aphodiid genus *Amidorus* includes more than 15 species, some of which are surely present in the Western Palearctic region (Dellacasa et al., 2001; Dellacasa and Dellacasa, 2006; Tarasov, 2008). Among these species, *A. immaturus* (Mulsant, 1842) is characterized by reduced distribution, being currently recorded from alpine localities of southeastern France (Nicolas and Riboulet, 1967; Piau et al., 1999), northwestern Italy (Jay-Robert et al., 1997; Tagliaferri, 2000; Dellacasa and Dellacasa, 2006), Switzerland, and Austria (Dellacasa and Dellacasa, 2006).

The rare *A. immaturus* was recognized as a species only recently (Nicolas and Riboulet, 1967; Paulian and Baraud, 1982; Piau et al., 1999; Tagliaferri, 2000). Since the features of this species are almost identical to those of other congeners, the taxonomic identification should not be based on external morphological characters (Dellacasa and Dellacasa, 2006). The male genitalia (the aedeagus) of *A. immaturus* show instead well-defined characters, e.g., the shape of paramers, that are clearly unmistakable, as remarked by many authors (Nicolas and Riboulet, 1967; Dellacasa, 1983; Tagliaferri, 2000; Dellacasa and Dellacasa, 2006). The female vaginal sac can be used as an identifying character at the subgeneric level (Tarasov, 2008), but not at a specific level.

Apart from the genitalia, the epipharynx also shows characteristic features (Dellacasa, 1983) and can therefore be usefully employed to identify the individuals at a

specific level irrespective of sex, since the structure does not display any sexual dimorphism (Tocco et al., 2011).

2. Materials and methods

During the summer of 2008, *Amidorus* adult specimens ($N_{TOT} = 219$) were collected from 3 sites in Ferret Valley (Valle d'Aosta, Italy), where *A. immaturus* is sympatric with *A. obscurus* (Palestrini et al., 2008b): Rifugio Elena (2070 m a.s.l., ED50 UTM 350075E 5083255N; 1970 a.s.l., ED50 UTM 349774E 5082171N; 1860 m a.s.l., ED50 UTM 3494625E 5082540N), Arpnouva-Greuvettaz (1770 m a.s.l., ED50 UTM 348995E 5081658N), and Lavachey (1660 m a.s.l., ED50 UTM 346901E 5079885N) (Figure 1).

The adults were collected by pitfall traps and direct collecting in dung pads. Employing glass jars filled with cow dung, live specimens were carried to the laboratory. To rear the larval instars, we put the adults in individual plastic containers in isolation (polyethylene glasses, 9.5 cm diameter, 12.5 cm height) with a cover. Soil was put on the bottom of the plastic container; it was then covered with fresh dung. Abundant food was supplied to avoid the potential risk of intraspecific competition among the siblings and the adult individuals in each terrarium.

The rearing process was carried out under laboratory conditions, and the room parameters (temperature mean = $23.20 \text{ }^\circ\text{C} \pm 0.60$ and humidity mean = $60.00\% \text{ RH} \pm 0.18$) were acquired by a datalogger HumiStick (TecnoSoft). The data were downloaded and read by the software UTM v1.2. (TecnoSoft).

* Correspondence: angela.roggero@unito.it



Figure 1. Map of Valle d'Aosta (Italy), with a black dot placed on the collection area.

After 4 weeks, the polyethylene glasses were opened to collect the larvae. Both adults and preimaginal instars were killed and stored in individual vials filled with 99% ETOH, in which the larvae were maintained until they were photographed. To avoid any misclassification we kept all the individuals separate and identified a posteriori the species and sex of the adult specimens.

To assign the larvae to the correct species, we examined the epipharynx of mothers, whose features were compared with the epipharynx of assuredly identified males on the basis of the genitalia characters (Tocco et al., 2011). Dissection and slide preparation of the epipharynx was performed according to the usual methods applied to coleopteran taxa (Dellacasa et al., 2010).

We acquired images of various anatomical parts (i.e. genital disc, head, thorax, abdomen) and of the whole body on the side view by the modular zoom system Leica Z16 APO microscope connected to a Leica DFC320 digital camera (Leica Microsystems AG). Measurements of the anatomical structures, i.e. the pygidium (Figure 2a), whole body (Figure 2b), head (Figure 2c), and thorax (Figure 2d), were then taken using the LAS (Leica® Application Suite) software v 2.5.0.

According to Brooks' (1886) and Dyar's (1890) hypothesis of a geometric progression of size measures during larval development, the discontinuous growth of various body parts in preimaginal instars (Hutchinson et al., 1997) was compared to the size of heavily sclerotized structures (i.e. the head capsule) that maintain approximately the same size during each instar and grow only at the molt. Dyar's rule is commonly applied to the head measures in preimaginal analyses, being considered a simple method to determine larval instars (Daly, 1985). We used the head width (H_Width) to create the frequency

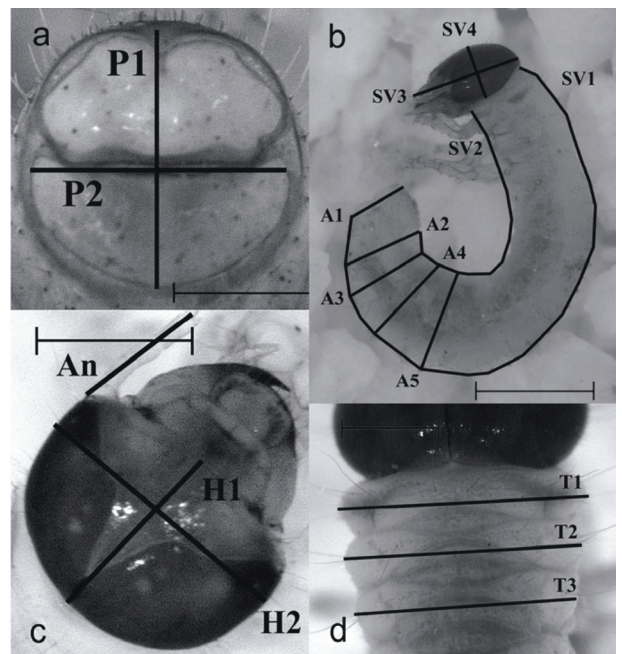


Figure 2. Measures: a) X abdominal segment, P1 = pygidium length, P2 = pygidium width; b) side view, SV1 = external length, SV2 = internal length, SV3 = head length to clypeus, SV4 = head width by side, A1–A5 = abdominal segments' width; c) head, An = antenna length, H1 = head length, H2 = head width; d) thorax, T1–T3 = thoracic width.

chart in order to assign individuals to the correct larval instar.

For each linear size measure, the growth ratio is defined by the values of 2 subsequent instars. Allometry (i.e. variation in growth ratio in different anatomical traits) in the larvae is a more common event than expected (Stern

and Emlen, 1999). To evaluate the growth ratio for each measure in the larvae, the mean sizes of 2nd larval instar were divided by the corresponding values of 1st larval instar.

In immature coleopteran stages, the genital imaginal disc constituted an area in the next-to-last abdominal segment showing a marked sexual dimorphism: along the midline, very distinct and well-defined in males; far less evident and placed on the side in females (Martínez and Lumaret, 2003, 2005). This structure can be used for larval sex determination in preimaginal instars, although it was employed only in a small number of Coleoptera until now (Moczek and Nijhout, 2002; Martínez and Lumaret, 2003, 2005). Once the sex of the larvae has been determined, the sex ratio can be evaluated as is usually done through the ratio of the numbers of males and females.

We also used ANCOVA to test whether the size variation of the larvae can be ascribed to sexual dimorphism, with sex as a fixed factor and instar as the covariate.

To examine whether the number of offspring of each nest could affect the dimensions of the preimaginal instars, we examined the body size variation using regression analysis. The head width (H_width, Figure 2c) was chosen as the measure of the overall size of the larvae (dependent variable).

All of the above analyses were performed with PASW Statistics v18 (IBM Corporation).

3. Results

In the experimental set-up we obtained a total of 90 larvae from 6 females of *A. immaturus* (mean = 15 larvae for each individual, standard deviation = ± 5.18).

The head width measures show a bimodal distribution of data, in which each mode is nevertheless characterized by a normal distribution, the 2 well-separated modes corresponding to 2 different instars of *A. immaturus* (Palestrini et al., 2009). Two distinct groups are evident for *A. immaturus*, which are then assigned to 1st and 2nd instars respectively by comparison with analogous results previously obtained by the analysis of the 3 preimaginal instars of *A. obscurus* (Fabricius, 1792) (Palestrini et al., 2009).

Differences in growth ratio (G_r) were found in different anatomical traits for this *Amidorus* species (Figure 2a), since the G_r of the measures of the head and antenna is about 1.4 but the G_r of other measures, such as the thorax or abdomen, is higher (Table 1). It can thus be hypothesized that the cephalic capsule is characterized by a lesser developmental pattern than the other anatomical traits during growth.

The genital disc is located in the penultimate abdominal segment and shows marked sexual dimorphism for each larval instar. According to the presence/absence of the

Table 1. Growth ratio values.

	Growth ratio
<i>H_Length</i>	1.46
<i>H_Width</i>	1.44
<i>Antenna</i>	1.48
<i>A_1</i>	1.79
<i>A_2</i>	1.77
<i>A_3</i>	1.90
<i>A_4</i>	1.94
<i>A_5</i>	1.92
<i>P_1</i>	1.76
<i>P_2</i>	1.63
<i>SV_1</i>	1.84
<i>SV_2</i>	1.73
<i>SV_3</i>	1.52
<i>SV_4</i>	1.46
<i>T_1</i>	1.57
<i>T_2</i>	1.65
<i>T_3</i>	1.65

genital disc, we could identify the sex of the larvae to evaluate the sex ratio as a whole and in the various instars. The sample of the larvae (N = 90) contained 47 females and 43 males, with a sex ratio value that approaches 1:1. Comparing the variation in size (i.e. the measures of the cephalic capsule) in different instars and sexes of *A. immaturus* (Table 2), it was determined that there are no significant differences for the size within the sexes in each larval instar.

In ANCOVA, the test of between-subject effects gave nonsignificant results for sex (F = 0.905, P = 0.344, and F = 0.008) as well as the mean pairwise comparison (Bonferroni adjusted) with P = 0.103. Through linear regression, no significant correlations were found between the number of offspring of each nest and the size of larvae (F = 0.003, P = 0.955).

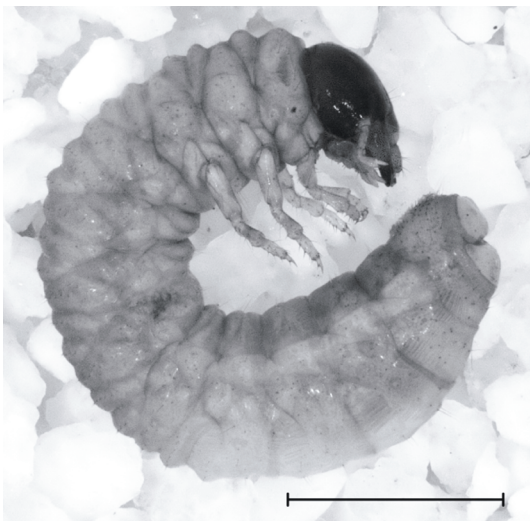
3.1. Description of the 1st and 2nd larval instar of *A. immaturus*

Material examined: ITALY: Valle d'Aosta, Val Ferret: Rifugio Elena; Arpnouva-Greuvettaz; Lavachey.

Larval 2nd instar: Total length (TL) = 5.09–10.10 mm (N = 40). Ivory-colored melolonthoid larva (Figure 3). Well-sclerotized, dark brown head; thoracic segment I wider than the other 2, which are subequal. Abdominal

Table 2. Measures of head in the 2 preimaginal instars, in males and females separately.

	♀♀				♂♂			
	Instar 1		Instar 2		Instar 1		Instar 2	
	H_Length	H_Width	H_Length	H_Width	H_Length	H_Width	H_Length	H_Width
N	24	24	23	23	26	26	17	17
Mean	0.61	0.89	0.88	1.28	0.61	0.90	0.89	1.30
Minimum	0.53	0.84	0.77	1.23	0.51	0.83	0.78	1.25
Maximum	0.69	0.96	0.99	1.33	0.68	0.94	1.02	1.35
Range	0.16	0.12	0.22	0.10	0.17	0.11	0.23	0.10
Std. deviation	0.04	0.03	0.07	0.03	0.05	0.02	0.07	0.03
Variance	0.002	0.001	0.004	0.001	0.003	0.001	0.005	0.001

**Figure 3.** Larva (2nd instar) of *A. immaturus*. Side view, scale bar = 2 mm.

segments V–VIII characterized by dorsal expansion. Thin, sparse, long, and evenly tawny pubescence that is arranged along a segmented, medial line on ventral side. The ventral medial pubescent line goes down to dorsal side with thicker bristles.

Head (Figure 4a). Width (HW) = 1.23–1.35 mm, length (HL) = 0.76–1.01 mm. Evenly well-sclerotized, wider than larger cephalic capsule, while mouthparts are unevenly sclerotized. Uneven pubescence, with 4 long setae bordering the antennae, 2 long setae on sides of the first part of epicranial suture, and minor pubescence sparse on surface.

Epicranial suture evident and large (Figure 4a). Frons clearly bilobed, with frontal crest bifid and half as long as the head length. The symmetrical frontal sutures arise from the proximal part of the frontal crest, sinuously extending to antennal scape.

Subtrapezoidal clypeus (Figure 4b), with largely rounded fore angles. Clypeus is more sclerotized at basal two-thirds (anteclypeus, length = 0.19 mm) than at distal third (postclypeus, length = 0.11 mm), dorsally carrying a sensillum and 3 setae on each side along the medial line, the central seta longer than the other 2. Clypeal suture evident, subrectilinear, more prominent and pointed on sides.

Mouthparts. Asymmetrical mandibles (Figure 4c and 4d) arched, more sclerotized at apex. Left mandible with 4 large, external setae, 2 at base, 1 in the middle of the surface, and 1 subapically near the incisure that circumscribes the spatulate area; molar area constituted by 2 structures, the superior part protruding roofing-like, and the inferior part forming a more evident crest along the left side; scissorial area spatuliform, arched, carrying a small tooth laterally. Right mandible with scissorial area arched and notched on side, with a large tooth, 4 setae on external side, 2 at base, 1 in the middle and 1 near the scissure. Concave and subquadrangular molar area, the right basal part asymmetrical. Longitudinal fringe of setae above the molar area. Tuft of setae on inner margin of both the mandibles, externally to molar area.

Maxillae (Figure 4e), characteristic swelling labaconia, with a long seta on posterior side and some others scattered. Cardo short (length = 0.23 mm, width = 0.23 mm), with

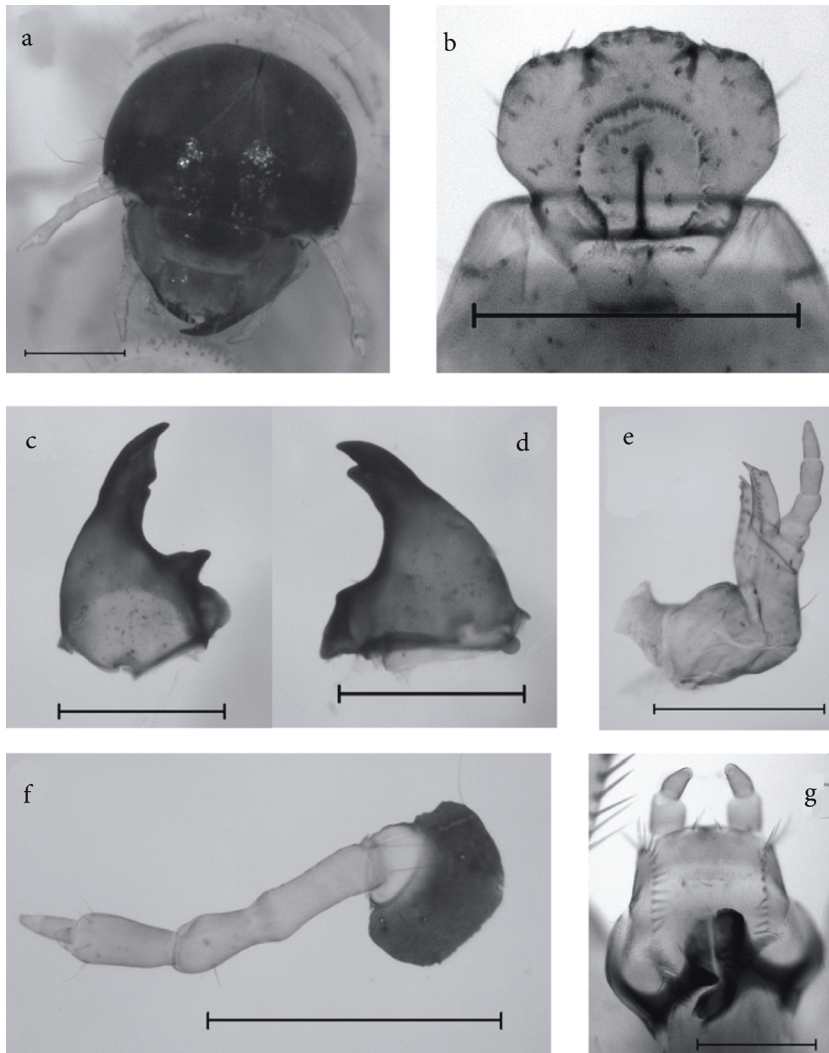


Figure 4. Larva of 2nd instar of *A. immaturus*: a) head, scale bar = 0.5 mm; b) epipharynx, scale bar = 0.5 mm; c) right mandible, ventral view, scale bar = 0.5 mm; d) left mandible, ventral view, scale bar = 0.5 mm; e) left maxilla, ventral view, scale bar = 0.5 mm; f) antenna, scale bar = 0.5 mm; g) hypopharynx, scale bar = 0.2 mm.

a long and thick seta in the middle. Stipes carrying a long seta on posterior side, and other setae scattered on surface; precoila with an oblique row of 9 stridulatory teeth, and 2 other teeth aside, near 2 setae toward the palpiger. Galea (length = 0.38 mm) greatly mucronate, with the point inwardly directed, with 5 sturdy setae regularly disposed in a row on the inner surface, a longitudinal row of 13 thick and short setae on outer surface. Lacinia (length = 0.33 mm) elongate, slightly curved, mucronate at apex, regularly bordered on inner margin by a longitudinal row of strong setae, 5 single and elongate, and 2 paired at apex, plus 2 setae on inner surface at base. Thin palpiger (length = 0.06 mm) bearing 4 maxillary palps (lengths = 0.08, 0.07, 0.08, 0.11 mm, respectively) that are subcylindrical except

the last 1, conical, well-sclerotized, and truncated at apex, with macrosensilla in a nonsclerotized area. Each palp bears a long and thin seta on external side. Penultimate palp carrying 2 setae and 2 proximal sensilla.

Labrum only slightly trilobed, with subequal lobes, and scarcely sclerotized, carrying 4 equidistant long and thick setae on a transversal medial row, a pair of proximal sensilla medially, and few minute and sparse setae.

Antennal scape (Figure 4f) short and desclerotized, 1st antennal joint elongate, cylindrical, 2nd antennal joint shorter and slightly enlarged at apex, 3rd antennal joint similar to former joint, but desclerotized at apex and carrying the laterally inserted, smaller 4th antennal joint cone-shaped frustum, with a basiconic sensillum. The 3rd

antennal joint carries subapically a circle of 6 setae, while the 4th has at apex a desclerotized small circular area and microsensilla with 2 minute setae.

Epipharynx (Figure 4b, maximum length = 0.34 mm, maximum width = 0.44 mm, length from clythra to base = 0.30 mm, width between clythra = 0.17 mm) largely trilobed, the central lobe well developed. Evident, triangular, and slightly asymmetrical clythra. Acropariae constituted by a double line of thick setae (4 short anteriorly and 4 longer), and 2 longer ones inserted posteriorly. Acanthopariae constituted by 7 setae from clythra to base, arranged as 2 small setae, 2 paired long setae, 2 paired small setae, and then a small single seta. At base, near the apotormae, chaetopariae constituted by a small single seta. Haptomerum carrying a pair of macrosensilla. Gymnopariae extended. Dexiophoba and laeophoba forming a subcircular pedial area. The oval pedium carrying in the middle an evident and rectilinear anterior epitorma, enlarged and rounded at apex. In pedial area there is also a short and irregular dexioprophoba. Pternotormae merged medially to form the base of epitorma. Apotormae small and slightly evident. Laeotorma and dextortorma asymmetrical, narrow, and slightly sclerotized.

Labium carrying 2 pair of setae, 1 near the base and the other on the midline.

Hypopharynx (Figure 4g, length = 0.30 mm, width = 0.38 mm) with evident, asymmetrical oncili. The Y-shaped right 1 extending caudally, the left 1 truncated at apex with a lamina elongate to anterior margin of hypopharynx. The labial palps with the 1st segment subcylindrical and larger (length = 0.06 mm) than the 2nd (length = 0.05), which narrows to apex, with macrosensilla and 2 setae. Inapparent palpiger, from which a longitudinal fringe, first regular and then irregular, of 22 setae arises to hypopharynx base, ending to maxillulae that are lateral to the oncili. Ligula and glossa separated by a transversal row of 19 sensilla. Ligula carrying 2 pairs of short setae and 4 macrosensilla.

Prementum and postmentum clearly separate and evident. Well-sclerotized area with 2 large setae by the side and 2 smaller setae nearer the center together with a pair of proximal macrosensilla.

Thorax. Thoracic segment I with a large sclerotized band expanded on sides, evident and subtriangular, narrowing in the middle. Dorsal pubescence with short setae in the middle and longer setae on sides of a sclerotized band. The spiracle of the 1st thoracic segment is more evident, carrying a small cribose and scarcely sclerotized plica, which is inapparent in 2 other segments.

Legs (Figures 5a–5c). Foreleg coxa shorter than in the 2 other legs (Table 3), trochanter desclerotized and narrow in the 3 leg pairs, with an ochreous, minute, and untidily sparse pubescence. Subrectilinear femur in the 3 pairs of legs. Unguicula with 2 thick setae inserted near a narrowing area, at ½ of the length.

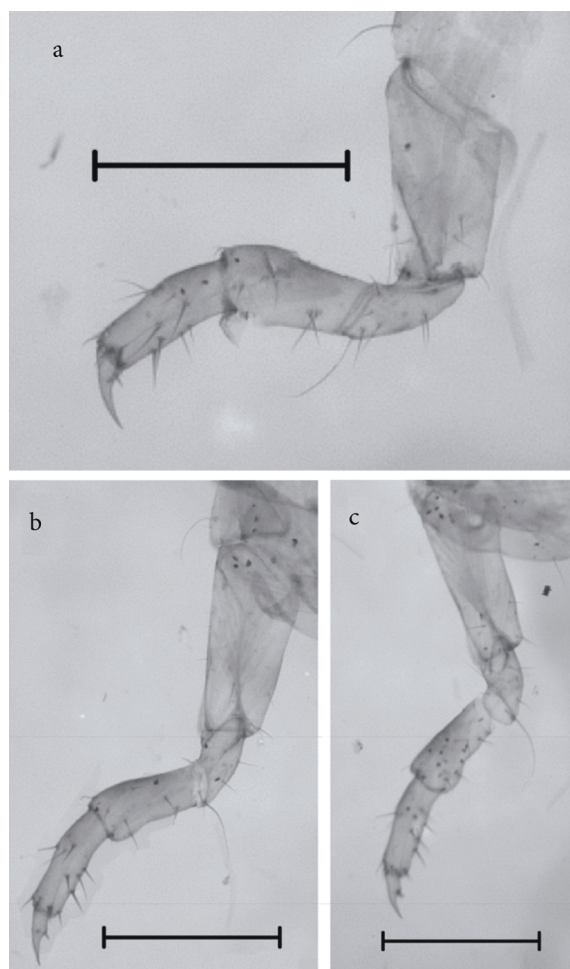


Figure 5. Legs of *A. immaturus* larva, scale bar = 0.5 mm: a) fore leg; b) medial leg; c) hind leg.

Abdomen. Spiracles almost inapparent, not sclerotized (Figure 3). In males, on the penultimate abdominal segment the genital disc (Figures 6a and 6b) is well defined, down-turned, triangular (almost cordiform) with a deep and large incisure on proximal margin, opalescent. The subcylindrical X abdominal segment with ventrally a raster (Figure 7a) constituted by short teges (or tegilla), and thick untidy setae (N = 52–53). On sides there are about 8 barbulae. Well-developed, glabrous campus with a pair of large setae caudally oriented. Anal lobe (Figure 7b) superior part semicircular, inferior part deeply notched forming 2 parts swollen and bilobed.

Larval 1st instar: Total length (TL) = 2.62–6.26 mm (N = 50). Ivory-colored melonothoid larva.

Head. Width (HW) = 0.83–0.95 mm, length (HL) = 0.51–0.68 mm.

The 1st larval instar is very similar to the 2nd instar. In both the instars the genital disc is present in males (Figures 6a and 6b), with some differences of features that were not quantified yet.

Table 3. Measures of the 2nd instar larva of *A. immaturus*.

	Measure	mm
Antenna	Scape	0.09
	Antennal joint I	0.22
	Antennal joint II	0.15
	Antennal joint III	0.18
	Antennal joint IV	0.10
	Basiconic sensillum	0.03
Leg I	Coxa	0.44
	Trochanter	0.20
	Femur	0.26
	Tibia	0.27
	Tarsus	0.16
Leg II	Coxa	0.49
	Trochanter	0.23
	Femur	0.32
	Tibia	0.27
	Tarsus	0.14
Leg III	Coxa	0.50
	Trochanter	0.24
	Femur	0.30
	Tibia	0.29
	Tarsus	0.16

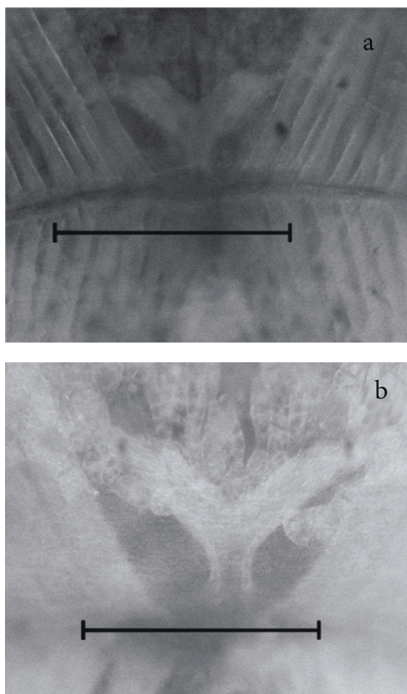


Figure 6. Genital disc of *A. immaturus* male, scale bar = 0.2 mm: a) 1st instar; b) 2nd instar.

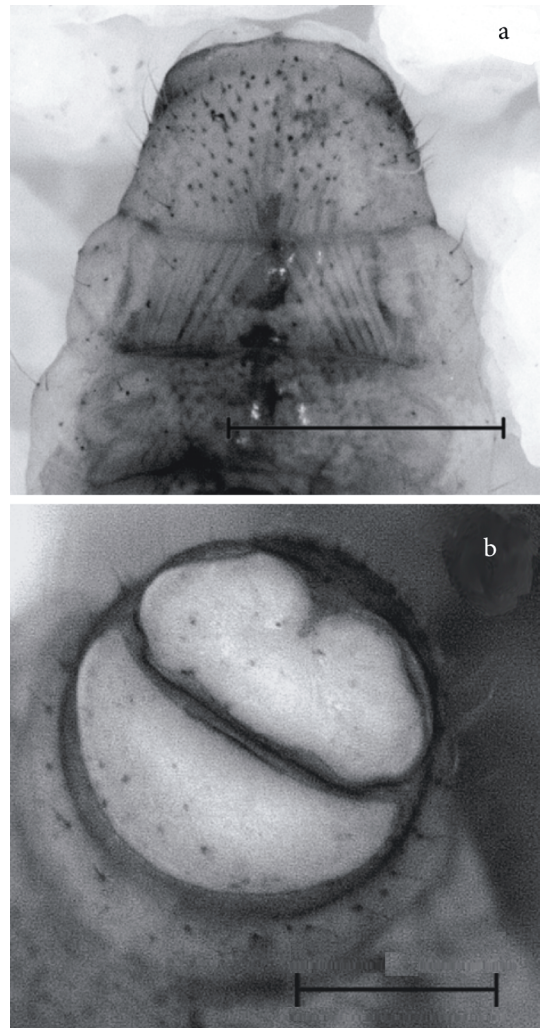


Figure 7. Larva of *A. immaturus*: a) raster, scale bar = 1 mm; b) X abdominal segment, scale bar = 0.5 mm.

The majority of the differences were evidenced in the measures of anatomical traits. The epipharynx (Figure 8, maximum length = 0.21 mm, maximum width = 0.29 mm, length from clythra to base = 0.19 mm, width between clythra = 0.11 mm) trilobed, the central lobe less developed than in 2nd instar. Differences were also present in the lateral lobes of epipharynx, which are less developed in 1st larval instar than in 2nd instar. Anteclypeus (length = 0.11 mm) and postclypeus (length = 0.08 mm) are almost identical in features to the 2nd instar.

All the other mouthparts are similar in the 2 instars, varying only in size. Maxillae (Figure 9) palpiger length = 0.05 mm; the 4 palps length = 0.05, 0.06, 0.05, 0.05, 0.09 mm. Lacinia length = 0.20 mm, galea length = 0.25 mm. Cardines length = 0.17 mm, width = 0.19 mm. Hypopharynx width = 0.24 mm, length = 0.18 mm.

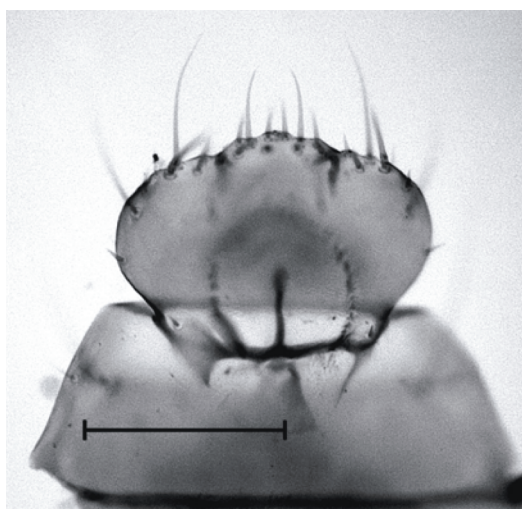


Figure 8. Epipharynx of 1st instar larva, scale bar = 0.2 mm.



Figure 9. Hypopharynx and maxillae of 1st instar larva, scale bar = 0.2 mm.

4. Discussion

As previously pointed out (Palestrini et al., 2008a), the aphodiid larval pattern did not greatly differ in distinct species, all being characterized by relatively constant morphological features. In *A. immaturus*, as recorded for many other species, the external morphological traits do not differ in the 2 sexes nor among the various larval instars. The preimaginal individuals increase in size with the characteristic discontinuous growth (corresponding to the various instars), and the size of the larvae is not related to the number of offspring of each nest or to the sex. The maintenance of a relatively simple pattern is effective for rapid development and is an obvious choice for species characterized by an R-strategy. Furthermore, rapid development that does not require the allocation of

many resources is surely the best choice for the high-quote species.

The aphodiid are for the most part endocoprid, but some species show a rudimental sort of nesting behavior, as it was observed that the larvae of *A. immaturus* can dig tunnels and move back and forth between the dung pad and the soil. Such behavior is usually displayed by high-quote mountainous species, in response to quick and massive lowering of temperature.

Acknowledgments

This study was supported by grants from the Italian Ministero dell'Istruzione, dell'Università e della Ricerca (MIUR). We would like to thank Dr Dan Chamberlain for the English text revision.

References

- Brooks, W.K. 1886. Report on the Stomatopoda collected by H.M.S. Challenger during the years 1873-76. Zoology Part XLV. In: Report of the Scientific Results of the Voyage of the H.M.S. Challenger during the Years 1873-76. H.M. Stationery Office, London (*partim*).
- Daly, H.V. 1985. Insect morphometrics. *Annu. Rev. Entomol.* 30: 415-438.
- Dellacasa, G. 1983. Sistematica e nomenclatura degli Aphodiini italiani (Coleoptera Scarabaeidae: Aphodiinae). Museo Regionale di Scienze Naturali di Torino.
- Dellacasa, G., Bordat, P. and Dellacasa, M. 2001. A revisional essay of world genus-group taxa of Aphodiinae (Coleoptera Aphodiidae). *Mem. Soc. Entomol. It.* 79(2000): 1-482.
- Dellacasa, G. and Dellacasa, M. 2006. Fauna d'Italia. XLI. Coleoptera. Aphodiidae, Aphodiinae. Calderini, Bologna.
- Dellacasa, G., Dellacasa, M. and Mann, D.J. 2010. The morphology of the labrum (epipharynx, ikrioma and aboral surface) of adult Aphodiini (Coleoptera: Scarabaeidae: Aphodiinae) and the implications for systematics. *Insecta Mundi* 132: 1-21.
- Dyar, H.G. 1890. The number of molts of lepidopterous larvae. *Psyche* 5: 420-422.
- Hutchinson, J.M.C., McNamara, J.M., Houston, A.J. and Vollerath, F. 1997. Dyar's Rule and the Investment Principle: optimal moulting strategies if feeding rate is size-dependent and growth is discontinuous. *Phil. Trans. R. Soc. B* 352: 113-138.

- Jay-Robert, P., Lobo, J.M. and Lumaret, J.P. 1997. Altitudinal turnover and species richness variation in European montane dung beetles assemblages. *Arctic Alpine Res.* 29: 196–205.
- Martínez, I.M. and Lumaret, J.P. 2003. Dimorfismo sexual en larvas de Scarabaeoidea (Coleoptera). In: *Monografías Tercer Milenio Vol. 3. Escarabeidos de Latinoamérica: Estado de conocimiento* (Eds. G. Onore, P. Reyes-Castillo, M. Zunino). SEA, Zaragoza, pp.15–18.
- Martínez, I.M. and Lumaret, J.P. 2005. Structure of the terminal ampulla in male larvae of *Canthon cyanellus* LeConte (Coleoptera: Scarabaeidae: Scarabaeinae). *Coleopt. Bull.* 59: 35–39.
- Moczek, A.P. and Nijhout, H.F. 2002. A method for sexing final instar larvae of the genus *Onthophagus* Latreille (Coleoptera: Scarabaeidae). *Coleopt. Bull.* 56: 279–284.
- Nicolas, J.L. and Riboulet, R. 1967. Les *Aphodius* Ill. français du groupe *obscurus* (F.). Le cas d'*immaturus* Muls. (Col. Scarabaeidae). *Bull. Mens. Soc. Linn. Lyon* 36: 113–117.
- Palestrini, C., Roggero, A. and Barbero, E. 2008a. The morphology of preimaginal stages of *Agoliinus satyrus* (Reitter, 1892) (Coleoptera: Aphodiidae: Aphodiini), with notes on reproductive biology. *Rev. Suisse Zool.* 115: 565–573.
- Palestrini, C., Roggero, A., Gorret, R., Tocco, C., Negro, M. and Barbero, E. 2008b. Scarabaeoidea coprofaga della Val Veny e della Val Ferret (Valle d'Aosta, Italia). *Rev. Val. Hist. Nat.* 61–62: 241–253.
- Palestrini, C., Roggero, A., Rolando, A. and Tocco, C. 2009. Morfometria larvale in *Amidorus obscurus* (F.) e *A. immaturus* (Mulsant) (Coleoptera, Aphodiidae). Atti 70° Convegno dell'U.Z.I., Rapallo (GE) 21-24.9.2009. *Boll. Mus. Ist. Biol. Univ. Genova* 71: 174.
- Paulian, R. and Baraud, J. 1982. Lucanoidea et Scarabaeoidea. Faune des coléoptères de France, 2nd ed. Lechevalier, Paris.
- Piau, O., Lumaret, J.P. and De Stordeur, E. 1999. Diversité et divergence de l'ADN mitochondrial d'*Aphodius obscurus* et *Aphodius immaturus* de France (Coleoptera: Aphodiidae). *Ann. Soc. Entomol. France* 35 (Suppl.): 117–123.
- Stern, D.L. and Emlen, D.J. 1999. The developmental basis for allometry in insects. *Development* 126: 1091–1101.
- Tagliaferri, F. 2000. Una specie nuova per la fauna italiana: *Aphodius (Amidorus) immaturus*. *Riv. Piem. St. Nat.* 21: 239–243.
- Tarasov, S.I. 2008. A revision of *Aphodius* Illiger, 1798 subgenus *Amidorus* Mulsant et Rey, 1870 with description of the new subgenus *Chittius* (Coleoptera: Scarabaeidae). *Russ. Entomol. J.* 17: 177–192.
- Tocco, C., Roggero, A., Rolando, A. and Palestrini, C. 2011. Inter-specific shape divergence in Aphodiini dung beetles: the case of *Amidorus obscurus* and *A. immaturus*. *Org. Divers. Evol.* 11: 263–273.